Nonlinear photonics in multidimensional and complex photonic lattices

C. Denz*[a], B. Terhalle[a,b], D. Göries[a], P. Rose[a], J. Xavier [a,c], T. Richter[d], A.S. Desyatnikov[b], J. Imbrock[a], T. J. Alexander[b], D.N. Neshev[b], J. Joseph[c], F. Kaiser[d], W. Krolikowski[b], Y.S. Kivshar[b]

[a]Institute for Applied Physics and Center for Nonlinear Science, Westfälische Wilhelms-Universität Münster, Germany.
[b]Nonlinear Physics Center and Laser Physics Center, Research School of Physics and Engineering, Australian National University, Canberra, ACT 0200, Australia.
[c]Photonics Group, Department of Physics, Indian Institute of Technology, New Delhi 110016, India.
[d]Institute for Applied Physics, Technische Universität Darmstadt, Germany.

ABSTRACT

We review some of our recent results on experimental light-induced periodic structures and their role in controlling light in discrete optics considering advanced features based on phase engineering and multiplexing of optically-induced lattices. While in the past only rather simple geometries like diamond, square, or hexagonal lattices were studied, we focus onto more complex photonic structures. Among them, we will present anisotropic triangular lattices, superlattices and three-dimensional lattices. We also study the propagation and localization of light in these structures – from simple waveforms to complex topological structures carrying phase dislocations.

Keywords: Nonlinear optics, refractive index changes, photonic lattices, gap solitons, optical vortices

1. INTRODUCTION

Due to versatile steering and control possibilities, wave propagation in nonlinear periodic structures has been the subject of extensive studies for several years. The interplay between periodicity and nonlinearity has been shown to cause a variety of fascinating nonlinear effects. In particular, discrete and gap spatial solitons have been studied in many different systems such as conjugated polymers [1], Bose Einstein condensates [2] and nonlinear waveguide arrays [3]. In optics, the induction of periodic refractive index structures in photorefractive materials [4] has been utilized to demonstrate a large variety of nonlinear localization effects such as soliton trains [5], Zener tunneling and Bloch oscillations [6] as well as vortex solitons [7–9]. The advantage of this induction technique is given by the electro-optic properties of photorefractive crystals such as strontium barium niobate (SBN), which allow highly nonlinear, reconfigurable refractive index patterns to be achieved at very low power levels. While in the past only comparatively simple geometries such as diamond, square [4,10,11] or hexagonal [12] lattices were studied, currently, special attention is paid to more complex photonic structures such as modulated waveguide arrays [13], lattice interfaces [14] or double-periodic 1d photonic lattices [15] as well as to the propagation of more complex waves as for example optical vortices or vortex solitons [16]. In general, complex or multiperiodic structures as well as complex wavefronts interacting with these lattices are of immense interest since they offer many exciting possibilities to engineer the diffraction properties of light. Among the many features that can be expected by these complex lattices, an example is the potential opening of additional mini gaps in the transmission spectrum, thereby paving the way to new soliton families in nonlinear media [17].

In this paper, we present several approaches to realize on the one hand complex two- and even three-dimensional photonic lattices, and on the other hand linear and nonlinear interaction with complex wavefronts carrying phase dislocations leading to novel stabilization mechanisms of complex waves.

2. WAVE PROPAGATION IN OPTICALLY-INDUCED PHOTONIC LATTICES

A simple and well-known procedure to generate a desired intensity distribution for optical induction of two-dimensional (2d) photonic lattices in photorefractive crystals utilizes the interference of several plane waves inside the biased photorefractive crystal [4]. The periodicity of the induced patterns can be controlled by the interference angle whereas the modulation depth depends on the externally applied electric field. More flexibility in changing the lattice parameters can

Nonlinear Optics and Applications III, edited by Mario Bertolotti, Proc. of SPIE Vol. 7354, 735402 · © 2009 SPIE · CCC code: 0277-786X/09/$18 · doi: 10.1117/12.823758

be achieved by using a programmable spatial light modulator to create the diffraction free propagating transversely periodic lattice wave [10,11]. For example, this configuration has been used to show the existence of discrete and dipole-mode gap solitons in photonic lattices of triangular shape [18] which would otherwise require the use of six plane waves and is consequently not very convenient to be induced by interference.

Mathematically, one can describe the optical induction of photonic lattices as well as beam propagation in these structures by the following set of equations:

$$2i\frac{\partial A}{\partial z}+\nabla_{\perp}^{2}A-\Gamma E_{sc}(I)A=0, \tag{1}$$

$$E_{sc}(I)=-\frac{\partial\varphi}{\partial x}, \tag{2}$$

$$\nabla^{2}\varphi+\nabla\varphi\nabla\ln(1+I)=E_{ext}\frac{\partial}{\partial x}\ln(1+I), \tag{3}$$

with $\nabla_{\perp}^{2}=\partial_{x}^{2}+\partial_{y}^{2}$. $\Gamma=k^{2}w_{0}^{2}n_{0}^{2}r_{eff}$ is proportional to the effective element of the linear electro-optic tensor r_{eff}. φ is the scalar potential of the electric screening field E_x and the externally applied electric field E_{ext} which is directed along the c-axis of the crystal. The total intensity I is the sum of the lattice wave and the probe beam intensity. Eq. (1) has been made dimensionless by introducing the length scales w_0 and $z_0 = kw_0^2$. k and n_0 denote the wave vector and the unperturbed refractive index, respectively. Throughout this paper, we use r_{eff} = 280 pm/V, n_0 = 2,35 and w_0 = 10µm.

Fig. 1 shows a schematic of a typical setup used in our experiments. A beam derived from a frequency-doubled Nd:YAG laser at a wavelength of 532 nm is split into two beams with adjustable intensities by using a combination of half wave plates and polarizing beam splitters. The transmitted beam illuminates a programmable spatial light modulator (SLM1) to imprint a phase modulation in such a way to create the desired non-diffracting lattice forming wave [10] necessary for the induction of periodic structures. The modulated beam is then imaged at the input face of a $Sr_{0.60}Ba_{0.40}Nb_2O_6$ (SBN:Ce) crystal by a high numerical aperture telescope. A half wave plate in front of the telescope is used to ensure ordinary polarization of the lattice wave, thus enabling its effectively linear propagation [4]. The crystal is additionally biased by an externally applied electric field and – to control the dark irradiance – uniformly illuminated with a white-light source. The second spatial light modulator (SLM2) combined with proper Fourier filtering is employed to achieve the desired amplitude and phase structure of an incident Gaussian probe beam. It is passed through a half wave plate to ensure its extraordinary polarization and subsequently sent to the CCD camera to record a phase interferogram with the probe beam. To observe the induced refractive index structure, the lattice can be illuminated with a broad plane wave, which is guided by the regions of high refractive index. As a consequence, the modulated intensity distribution at the output of the crystal qualitatively maps the induced refractive index. When including a Fourier-transform lens, the spectrum of the lattice can be analyzed too. A further analysis can be achieved by Brillouin zone spectroscopy [25,26].

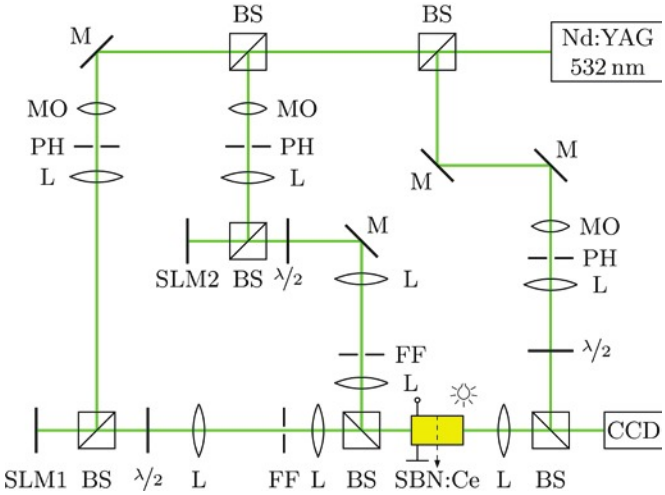

Fig. 1: Experimental setup. BS: beam splitter, CCD: camera, FF: Fourier filtering, L: lens, M: mirror, MO: microscope objective, PH: pinhole, SLM: spatial light modulator

3. TRIANGULAR LATTICES

For optically-induced lattices in photorefractive media, the induced refractive index change depends strongly on the anisotropy of the photorefractive response as well as on the polarization of the lattice wave [10,11,19]. In particular, its spatial orientation with respect to the c-axis of the crystal determines the symmetry of the resulting refractive index lattice, which can be different from the inducing light pattern. Even when considering lattices with a fourfold symmetry as the simplest example of highly symmetric structures, two lattice orientations can be distinguished: a square pattern with one high-symmetry axis orientated parallel to the c-axis, and a 45° tilted, so-called diamond pattern as it has been used in most experiments up to now. We have demonstrated that, due to the photorefractive anisotropy, the square lattice results in an effectively 1d refractive index structure consisting of vertical lines, whereas the induced refractive index change for the diamond pattern contains well separated spots, thus forming a fully 2d structure [10,11]. Furthermore, the anisotropic structure of the induced refractive index change has been shown to influence the symmetry of discrete solitons [19]. Due to the effectively 1d refractive index modulation, discrete solitons generated in the square lattice resemble 2d solitons in a quasi 1d lattice potential whereas a probe beam in the diamond lattice follows the dynamics known for truly 2d lattices.

Recently, we have extended the concept of solitons in optically induced lattices to more complex anisotropic lattices and demonstrated, that with a concise analysis of the non-diffracting patterns in the anisotropic photorefractive material the formation of more complex and higher-order discrete and gap solitons is possible. As an example of an anisotropic photonic structure, we have chosen complex triangular lattices with

$$A_{latt}(X,Y) = \hat{A}_{latt} \sin\left(\frac{2Y}{\sqrt{3}}\right) \sin\left(\frac{Y}{\sqrt{3}} + X\right) \sin\left(\frac{Y}{\sqrt{3}} - X\right). \tag{4}$$

As shown in Fig. 2, we distinguish two different orientations of the lattice wave: the so-called parallel orientation with *(X,Y) = (x,y)* and the perpendicular orientation with *(X,Y) = (y,x)*. For the parallel orientation (top row in Fig. 2), the output of a guided plane wave (Fig. 2(c)) reveals a fully 2d structure, while for the perpendicular orientation it contains vertical lines resembling an effectively 1d refractive index structure (Fig. 2(f)). In fact, these two lattices not only represent an example of highly-symmetric patterns that are transformed into lattices with reduced symmetry, but also patterns that are an extension of the commonly known fourfold symmetry diamond or square lattices. Triangular lattices in parallel orientation are higher-order lattices consisting of dipole structures oriented in a diamond pattern with angles of 60°. In particular, we have shown that the symmetry of discrete solitons in these lattices is influenced by the photorefractive anisotropy in a very similar way as in lattices with fourfold symmetry. The triangular lattice in parallel orientation in addition enables the formation of dipole-mode gap solitons [18].

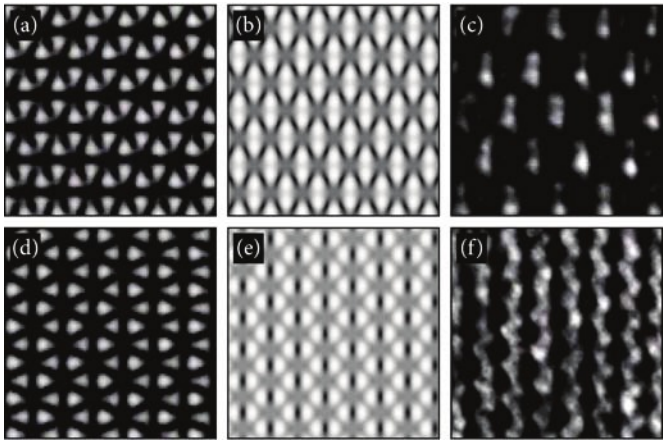

Fig. 2: Parallel (top) and perpendicular (bottom) triangular pattern. (a, d) Lattice wave, (b, e) numerical simulation of the light-induced refractive index change, (c, f) guided wave

In Figs. 3 and 4, we summarize our experimental and numerical results on the existence of solitons in such triangular lattices. It is clearly visible that the diffraction of the probe beam in the parallel oriented lattice at low power shows a behavior similar to the diamond lattice, forming a fully 2d diffraction pattern (Figs. 3(a, b)). In contrast, corresponding images for the perpendicular lattice (Figs. 3(g, h)) show an effectively 1d diffraction pattern consisting of vertical stripes

as observed for the square pattern [10,11]. Increasing the power of the probe beam, we observe the evolution from the described diffraction pattern to the strongly localized discrete solitons (Figs. 3(e, f) and (k, l)). The numerical simulations are in very good agreement with our experimental observations.

It has also been demonstrated that the lattice in parallel orientation with its dipole-like islands of high refractive index gives rise to the formation of dipole-mode gap solitons. By generating a dipole-like input, we were able to obtain a stable dipole-mode gap soliton (Figs. 4(c, f)). The existence of these stable solitons in triangular lattices offers novel possibilities to control dipole-like beams. In bulk photorefractive media they are known to experience strong repulsion [20], whereas in the presence of the lattice they are confined in one dipole-like island of high refractive index.

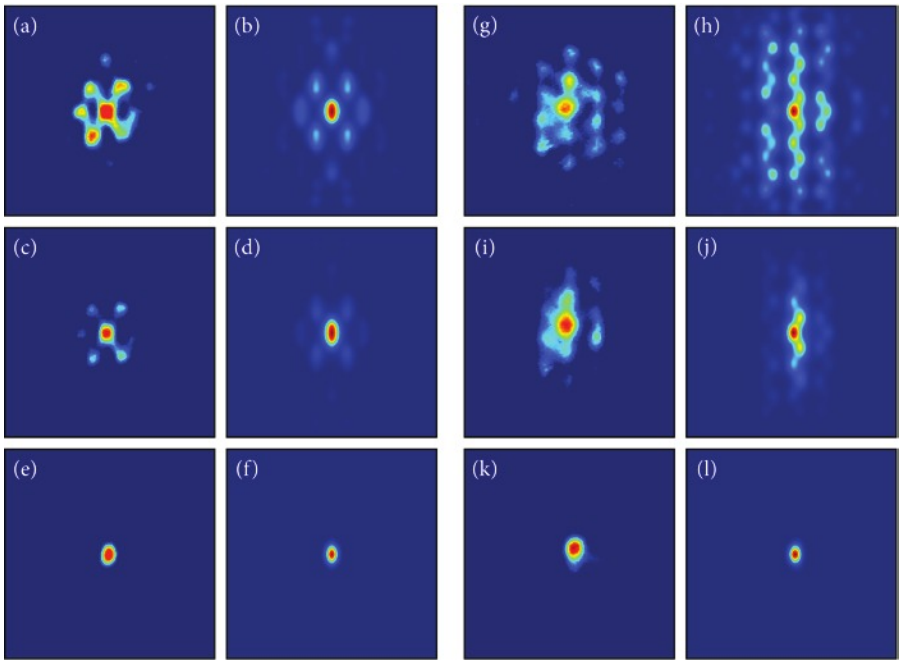

Fig. 3: Formation of fundamental discrete solitons in the parallel (a-f) and perpendicular (g-l) triangular lattice. First and third column show experimental results while second and fourth column depict the corresponding numerical simulations. (a, b), (g, h) Diffraction of the probe beam at low power (≈ 20 nW), (c, d), (i, j) localized state at moderate power (≈ 40 nW), (e, f), (k, l) discrete soliton (≈ 150 nW)

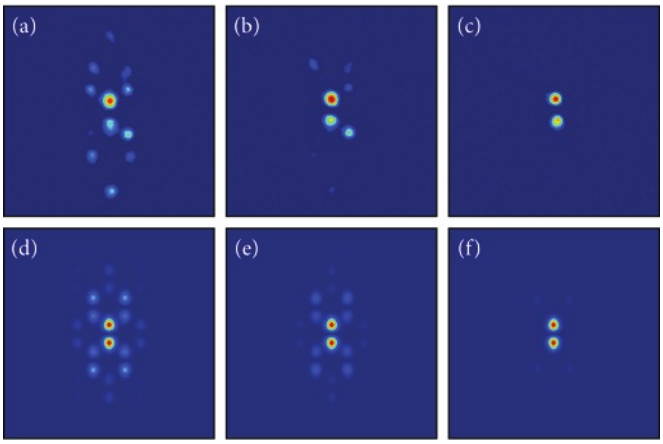

Fig. 4: Experimental results (top) and numerical simulations (bottom) for the formation of a dipole-mode gap soliton in the parallel triangular lattice. (a, b) Diffraction of the probe beam at low power (≈ 10 nW), (c, d) localized state at moderate power (≈ 25 nW), (e, f) dipole-mode gap soliton (≈ 90 nW)

4. SUPERLATTICES BY HOLOGRAPHIC MULTIPLEXING

At a first glance, superimposing lattices with different periodicities seems to be straightforward when employing the above-mentioned techniques. However, unfortunately, for the induction of multiperiodic lattices, the self-evident idea to use the spatial light modulator for a direct modulation of the lattice wave with a corresponding pattern is not successful. The reason is that lattice waves of different periodicities acquire different phase shifts during propagation and their coherent superposition therefore leads to an intensity modulation in the propagation direction due to interference. Consequently, a method of incoherent superposition is required. Of course a simple overlay of multiple incoherent interference patterns is feasible but lacks the flexibility benefits offered by the usage of a modulator.

A solution can be found when using multiplexing techniques known from holographic data storage. Several different approaches such as wavelength, angular and phase code multiplexing [21-23] allow the superposition of different refractive index patterns inside the volume of a photorefractive crystal and can serve as a basis for the induction of multiperiodic photonic superlattices. Compared with the commonly used sequential recording scheme, the method of incremental multiplexing [24] offers the possibility to induce the superimposed lattices with varied modulation depths by simply adjusting their relative illumination times. In fact, this enhances the flexibility of the induction process even more.

We have implemented this method for the induction of 2d diamond patterns of the form

$$A_{latt}(x,y) = \hat{A}_{latt} \sin\left(\frac{x+y}{\sqrt{2}}\right)\sin\left(\frac{x-y}{\sqrt{2}}\right). \tag{5}$$

In our experiments, we have analyzed the induced refractive index structures in Fourier space using Brillouin zone spectroscopy [25, 26]. If only one lattice period is used during the induction process, the Brillouin zone pictures show the corresponding lines marking the borders of the first Brillouin zone of the corresponding lattice (Figs. 5(d, e)). The induction of a 2d photonic superlattice as a superposition of these two structures is depicted in Figs. 5(c) and (f). The arrows in Fig. 5(c) indicate the alternating sequence of the two single periodic lattice waves. Both waves are sent onto the crystal in an alternating scheme having the same power, respectively. It is important to note that this illumination time is at least one magnitude smaller than the typical dielectric relaxation time of the used crystal, which at these intensities typically is in the range of tens of seconds. Fig. 5(f) clearly shows the Brillouin zone structure of the double-periodic 2d superlattice induced by the superposition of the two single periodic structures.

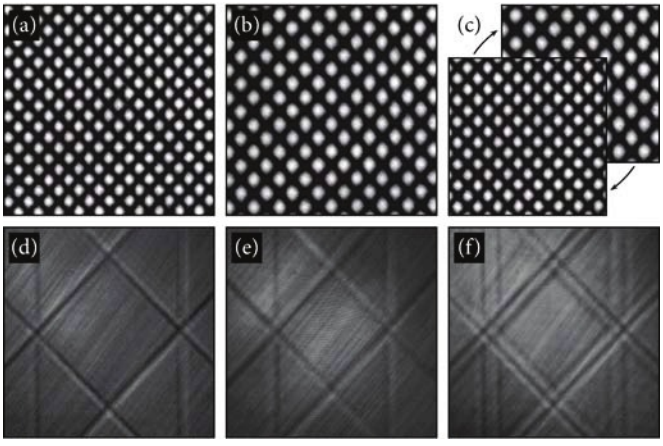

Fig. 5: Lattice wave (top) and Brillouin zone spectroscopy (bottom) of a 2d multiperiodic lattice. (a, d) Diamond pattern with lattice period of 17μm, (b, e) diamond pattern with lattice period of 28μm, (c, f) incremental multiplexing of diamond patterns with lattice periods of 17 and 28μm

We emphasize that the only fundamental restriction on the successively multiplexed structures is their diffraction free propagation through the medium. Therefore, the method of holographic multiplexing may also be extended to induce more sophisticated refractive index structures, for example asymmetric lattices being a superposition of many single periodic lattices of different symmetries.

5. VORTEX CLUSTERS

Some of the most spectacular observations of nonlinear dynamics of coherent light waves in periodic potentials relate to the properties of vortices and vortex flows in optical lattices [27-30]. Dramatic changes of light diffraction or tunneling of matter waves in media with periodically modulated parameters indicate novel directions for manipulating waves with a complex phase structure. Self-trapped phase singularities [16] in the form of isolated discrete vortices have been predicted theoretically [31-34] and generated experimentally in square photonic lattices [27, 28, 35].

We have investigated the stability properties of vortex clusters, i.e. clusters of weakly coupled fundamental solitons with a superimposed phase structure containing one or more phase singularities. In particular, we have demonstrated the existence of multivortex solitons [9] as well as double charge discrete vortex solitons [37] in hexagonal photonic lattices.

5.1 Multivortex solitons

Multivortex coherent states appear naturally in the systems with repulsive inter-particle interactions where they can be confined by external potentials. For attractive interaction, multivortex structures are known to be unstable, and they have only been observed as infinite periodic waves [11]. As a result, spatially localized multivortex states remain unobserved and largely unexplored. Recently it was predicted theoretically [37] that photonic lattices with threefold symmetry can support stable multivortex spatially localized states, in a sharp contrast to earlier studied square lattices [38]. Recently, we have reported on the experimental observation of topologically stable spatially localized multivortex solitons generated in optically-induced hexagonal photonic lattices [9] which can be described by

$$A_{latt}(x,y) = \hat{A}_{latt}\left(\exp\left(\frac{2ik_x x}{3}\right) + \exp\left(-\frac{ik_x x}{3} + ik_y y\right) + \exp\left(-\frac{ik_x x}{3} - ik_y y\right)\right). \quad (6)$$

The experimental observation of these structures is challenging due to the intrinsic anisotropy of the photorefractive nonlinear crystal, the induced potential is also strongly anisotropic [18]. To compensate for the asymmetry of the lattice and balance corresponding energy flows between the individual sites, the lattice is deformed from its exact hexagonal symmetry in such a way that the ratio of the spatial frequencies is changed from $k_x / k_y = \sqrt{3}$ to $k_x / k_y = 2.2$ resulting in a hexagonal structure which has been slightly stretched along its vertical direction.

To generate a multivortex probe beam, we focus three extraordinarily polarized beams onto the front face of the crystal in such a way that they have the same symmetry as the induced lattice. In the real space depicted in Fig. 6(a), this arrangement results in an input probe beam having the form of seven distinctive spots forming a hexagonal pattern with the same periods as the lattice and containing six vortices. At low input powers of ≈20 nW, the diffraction of the probe beam leads to a broad output distribution as shown in Fig. 6(b).

However, at high powers (≈1 μW), the structur e becomes localized and the output intensity distribution features seven well-pronounced spots closely resembling the input. To show the topological structure of multivortex solitons, we record the phase interferograms of the reference beam and the probe beam at low and high intensities, respectively. It is clearly visible that at low power (in the linear regime) the initial phase profile becomes strongly distorted. While the six initial vortices can still be found in the output field, their positions are changed. In contrast, for high input power of the probe beam (Figs. 6(c, f)) in the nonlinear regime not only the beam intensity becomes self-trapped but also the phase profile (Fig. 6(f)) retains exactly the same hexagonal vortex pattern of the input beam. We emphasize that the observation of stable multivortex solitons requires stretching of the photonic lattice. The reason for this behavior can be found in the intensity transfer between two lobes i and j. Under the assumption that all the lobes of the cluster are centered on the lattice sites and only weakly coupled, this intensity transfer can be derived as $J_{ij} \propto c_{ij} \sin(\phi_j - \phi_i)$ wherein $\phi_{i,j}$ denotes the respective phases, and c_{ij} are the coupling coefficients [9]. In order to create a stable vortex cluster, the intensity flows between all lobes should be balanced, i.e., $\sum_{i=1}^{N} J_{ij} = 0$ (see details in Ref. [38]).

For a structure with N = 7 and a hexagonal symmetry, this implies that the transverse power flow between each outer lobe and the center lobe has to be twice as high as those between the outer lobes themselves. Under this constraint the flow condition can be fulfilled only if for all adjacent lobes the coefficients c_{ij} become equal. However, this condition cannot be fulfilled in the case of hexagonal lattices with $k_x / k_y = \sqrt{3}$ due to the photorefractive anisotropy.

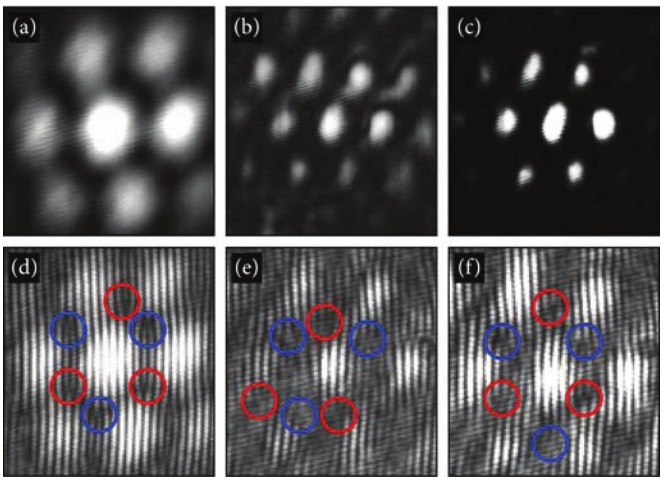

Fig. 6: Intensity distributions (top) and phase interferograms (bottom) of a multivortex soliton in a hexagonal lattice. Positions of the vortices are indicated by blue circles for the topological charge m = -1 and red ones for m = +1. (a, d) Probe beam input, (b, e) output intensity at low power, (c, f) multivortex soliton

As a result, at low powers of the input beam the anisotropic discrete diffraction dominates the dynamics. In the soliton regime the intensity of the probe beam attains a well defined 7-lobe structure but with an additional modulation resembling that of the diffracted beam. This modulation indicates complex deformations of the power flow [38]. Hence, in a hexagonal lattice, the vortices are unstable and undergo topological transformations during propagation. However, the photorefractive anisotropy of the lattice can be compensated for and, consequently, the energy flow can be balanced by adjusting the ratio k_x / k_y appropriately. Indeed, a stable phase profile can be achieved for the 7-lobe cluster in this case.

For a structure with N = 7 and a hexagonal symmetry, this implies that the transverse power flow between each outer lobe and the center lobe has to be twice as high as those between the outer lobes themselves. Under this constraint the flow condition can be fulfilled only if for all adjacent lobes the coefficients c_{ij} become equal. However, this condition cannot be fulfilled in the case of hexagonal lattices with $k_x / k_y = \sqrt{3}$ due to the photorefractive anisotropy. As a result, at low powers of the input beam the anisotropic discrete diffraction dominates the dynamics. In the soliton regime the intensity of the probe beam attains a well defined 7-lobe structure but with an additional modulation resembling that of the diffracted beam. This modulation indicates complex deformations of the power flow [38]. Hence, in a hexagonal lattice, the vortices are unstable and undergo topological transformations during propagation. However, the photorefractive anisotropy of the lattice can be compensated for and, consequently, the energy flow can be balanced by adjusting the ratio k_x / k_y appropriately. Indeed, a stable phase profile can be achieved for the 7-lobe cluster in this case.

5.2 Double-charge discrete vortex solitons

Lattices with a non-square symmetry such as hexagonal and honeycomb lattices show striking new vortex forms, including multi-vortex localized states [9, 37]. However, perhaps the most counter-intuitive result to emerge from the consideration of hexagonal lattices is that in the simplest six-site configuration double-charge vortices may become stable, while single-charge vortices are always unstable [39], in agreement with the stability properties of vortex solitons in modulated Bessel lattices [40]. This is particularly surprising as higher-charge discrete vortices are typically unstable in homogeneous nonlinear systems [16].

Here, we demonstrate experimentally the stability of a double-charge vortex in contrast to the corresponding single-charge vortex state which is unstable under the same conditions. As described in section 2, the lattice is formed with the help of one spatial light modulator. We use the second phase modulator to impose either a 2π or 4π phase winding on an input modulated (six-site) beam for the generation of single- and double-charge vortices, respectively. The characteristics of the beams are otherwise identical, and thus differences in the dynamics are due solely to the different input phases. We selectively vary the beam intensity to effectively move from the linear regime (low power, $I_{probe} \approx 50$ nW) to the nonlinear regime (high power, $I_{probe} \approx 550$ nW).

The single-charge vortex input is shown in Fig. 7(a). Its intensity distribution has a form of a necklace with six intensity peaks whose positions correspond to the lattice sites (index maxima). At low input power the beam undergoes discrete diffraction and a complete loss of the initial six site input state (Fig. 7(c)). At high power the initial six site intensity profile changes significantly after propagation (Fig. 7(e)), showing strong intensity modulations and even filling in the central lattice site. Furthermore, in the phase profile multiple vortices are seen to appear, further indicating a breakdown of the single-charge state (circles in Fig. 7(f)). We were unable to find an example of stable propagation of the single-charge vortex in the high-power (nonlinear) regime, a result consistent with the isotropic case predictions [39]. In the case of the double-charge vortex (Fig. 7(g-l)), we again observe a discrete diffraction with low input power (see Fig. 7(i)), however the result changes dramatically when the power is increased (see Fig. 7(k)). We observe that now the six-site input structure is preserved in the nonlinear propagation.

Interestingly, while the overall phase winding is still 4π, it can be clearly seen that the initial double-charge singularity has split into two single-charge vortices. This splitting of the higher-order singularity has been shown to be due to an inherent topological instability in the higher phase-winding. This topological breakdown in the linear (low power) part of the field further indicates that the stability of the 4π phase winding across the six sites is due to the interplay of the nonlinearity and local phase of the high-power sites suppressing the development of a dynamical instability. However, we find that this stability is critically dependent on the symmetry of the lattice, with a decrease in the lattice stretching (and thus a corresponding decrease in the symmetry of the underlying modulated refractive index) leading to a dynamical instability in the double-charge state as well.

The phase interferogram in Fig. 7(l) also indicates an additional pair of single-charge vortices of the opposite charge inside the vortex structure (not marked by circles). However, this additional pair does not affect the stability of the 4π phase winding, and it can be fully attributed to inevitable experimental noise in this region of low intensity of light.

To corroborate our experimental results, we have performed numerical simulations using the full anisotropic model as desribed in section 2. First we consider the case of a six-site initial state with a single-charge vortex phase of the form shown in Fig. 8(a) with either low or high power propagating a distance of 20 mm in the lattice. For the low input power case (Fig. 8(c)) we see that, as in the experiment, the vortex beam undergoes diffraction. If instead a high input power is considered (Fig. 8(c)) the vortex maintains much of its form.

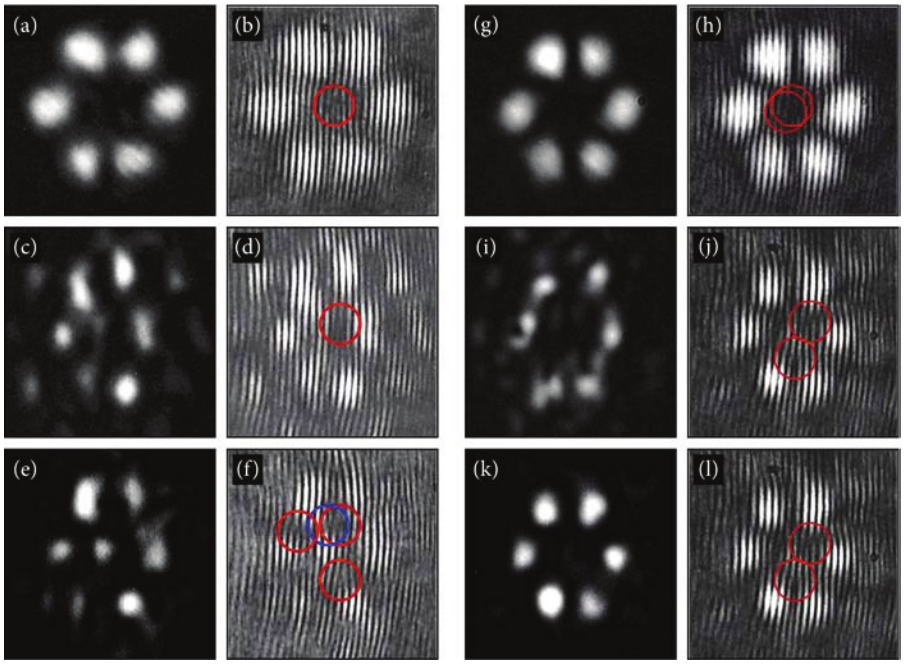

Fig. 7: Comparison of the stability of single- (a-f) and double-charge (g-l) vortices. Circles indicate positions of vortices with topological charge m=+1 (red) or m=-1 (blue). (a, b) Intensity and phase distribution of an input single-charge vortex beam, (c, d) beam profile and phase at the output for low input power, (e, f) output for high input power, (g, h) double-charge vortex input. (i, j) discrete diffraction for low power, (k, l) discrete double-charge vortex soliton.

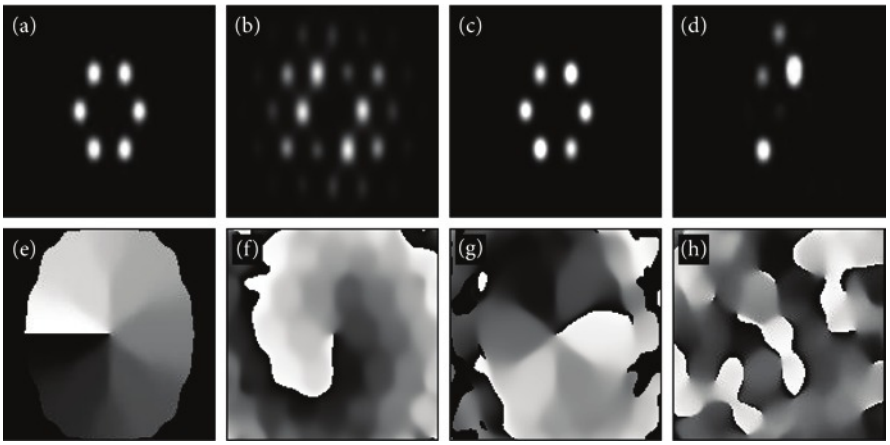

Fig. 8: Numerical simulation of the intensity (top) and phase profile (bottom) for a single-charge vortex. (a, e) Input, (b, f) beam profile at z = 20 mm for low input power, (c, g) beam profile at z = 20 mm for high input power, (d, h) high power output at z = 280 mm

Some intensity fluctuations are evident, and more importantly, the vortex phase has deteriorated showing breakdown of the initial single-charge vortex circulation. It must be noted that the break-up is clearly less than that observed in the experiment and this discrepancy is attributed to the higher anisotropy of the experimental lattice leading to a larger instability growth rate. In our numerical simulations, the strong instability becomes evident for longer propagation distances as shown in Fig. 8(d) for $z = 280$ mm.

In Fig. 9, we consider the same input beam intensities but change the phase to that of a double-charge vortex. The low power output (Figs. 9(b, f)) appears similar to the single-charge case, exhibiting diffraction and break-up of the vortex. In contrast, the high power output in Figs. 9(c-h) appears unchanged in the intensity profile with a well-pronounced double-charge vortex phase. Similar to the experimental results, the separation of the double-charge phase singularity into two single-charge singularities is observed. However the phase circulation around a contour tracing the six high intensity sites is well defined and equals 4π.

These results demonstrate experimentally and numerically the formation of stable double-charge vortex solitons in a hexagonal photonic lattice created optically in a self-focusing photorefractive crystal. In contrast, single-charge vortices are unstable in the same regime. Let us note again the importance of balancing the nonlinear anisotropy by stretching the lattice. Beyond a critical imbalance no stable double-charge vortices exist.

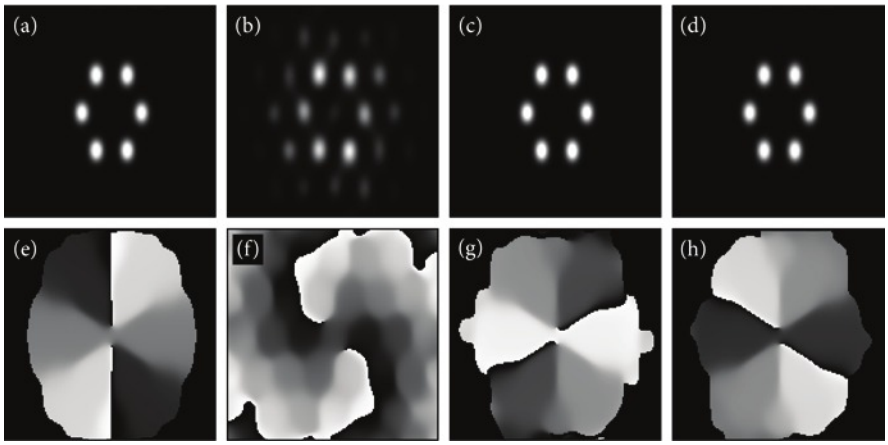

Fig. 9: Numerical simulation of the intensity (top) and phase profile (bottom) for a double-charge vortex. (a, e) Input, (b, f) beam profile at z = 20 mm for low input power, (c, g) double-charge discrete vortex soliton at z = 20 mm, (d, h) double-charge discrete vortex soliton at z = 280 mm

6. THREE-DIMENSIONAL LATTICES

Whereas 2d reconfigurable photorefractive lattices have become already quite well-understood and show – as we demonstrated above – fascinating effects of complex nonlinear physics as dipole or vortex soliton stability, three-dimensional (3d) reconfigurable structures that are able to show advanced nonlinear features as e.g. slow and stopped light have not been realized up to now.

Theoretically, it has been shown that by the interference of multiple beams as well as by the multiple exposure of two beam interference, all fourteen three-dimensional Bravais lattices could be generated [41, 42]. When this technique is adapted to the use of spatial light modulators, it can be significantly simplified. Here, we report the generation of well-defined reconfigurable three-dimensional (3d) nonlinear photonic lattices in externally biased strontium barium niobate (SBN:Ce) crystals by a single step optical induction approach.

As the photonic lattices in higher spatial dimensions influence the inter-site coupling and wave scattering in anisotropic media drastically, we experimentally explore the versatility of the optical induction approach for the fabrication of large area reconfigurable 3d structures with flexible parameters in such media.

Fig. 9 shows in the upper row computer simulations of the light intensity distribution obtained by the interference of the lattice forming beams, whereas the lower row shows the corresponding experimental results of a plane wave propagating in the structure in the direction indicated, revealing the refractive index modulation in this direction. The three-dimensional nature of the structure is clearly revealed.

The experimental analysis of these reconfigurable 3d structures proves their embedded potential in the area of nonlinear light-matter interaction investigations. The intrinsic nonlinear light localization in such structures and propagation of discrete modes in higher dimensions would give rise to the realization of promising nonlinear applications. In view of actual nonlinear photonic device integration in the technological quest for the realization of all optical active devices, we envisage the investigation of many exciting nonlinear propagation, trapping, switching, and steering beam dynamics in these highly reconfigurable 3d photonic lattices.

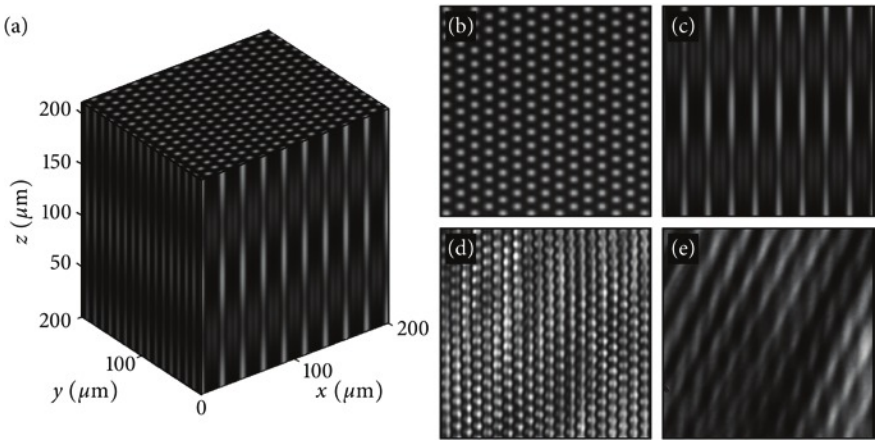

Fig. 10: Computer simulation of the light intensity distribution by the interference of lattice forming beams (a-c) and experimentally observed waveguiding (d, e). (a) three-dimensional interference pattern, (b, d) x-y plane, (c, e) x-z plane

ACKNOWLEDGEMENTS

Part of this work was support by the German Academic Exchange Service DAAD in the frame of the PhD exchange program with Australia and the sandwich PhD program with India.

REFERENCES

[1] Su W.P., Schieffer J R., Heeger A.J., "Solitons in polyacetylene", Phys. Rev. Lett. 42, 1698 (1979).

[2] Trombettoni A., Smerzi A., "Discrete solitons and breathers with dilute Bose–Einstein condensates", Phys. Rev. Lett. 86, 2353 (2001).

[3] Christodoulides D.N., Joseph R.I., "Discrete self-focusing in nonlinear arrays of coupled waveguides", Opt. Lett. 13, 794 (1988).

[4] Fleischer J.W., Segev M., Efremidis N.K., Christodoulides D.N., "Observation of two-dimensional discrete solitons in optically induced nonlinear photonic lattices", Nature 422, 147 (2003).

[5] Chen Z., Martin H., Eugenieva E.D., Xu J., Bezryadina A., "Anisotropic enhancement of discrete diffraction and formation of two-dimensional discrete-soliton trains", Phys. Rev. Lett. 92, 143902 (2004).

[6] Trompeter H., Krolikowski W., Neshev D.N., Desyatnikov A.S., Sukhorukov A.A., Kivshar Y.S., Pertsch T., Peschel U., Lederer F., "Bloch oscillations and Zener tunneling in two-dimensional photonic lattices" Phys. Rev. Lett. 96, 053903 (2006).

[7] Neshev D.N., Alexander T.J., Ostrovskaya E.A., Kivshar Y.S., Martin H., Makasyuk I., Chen Z., "Observation of discrete vortex solitons in optically induced photonic lattices", Phys. Rev. Lett. 92, 123903 (2004).

[8] Fleischer J.W., Bartal G., Cohen O., Manela O., Segev M., Hudock J., Christodoulides D.N., "Observation of vortex-ring 'discrete' solitons in 2D photonic lattices", Phys. Rev. Lett. 92, 123904 (2004).

[9] Terhalle B., Richter T., Desyatnikov A.S., Neshev D.N., Kaiser F., Krolikowski W., Denz C., Kivshar Y.S., "Observation of multivortex solitons in photonic lattices", Phys. Rev. Lett. 101, 013903 (2008).

[10] Desyatnikov A.S., Neshev D.N., Kivshar Y.S., Sagemerten N., Träger D., Jägers J., Denz C.,Kartashov Y.V., "Nonlinear photonic lattices in anisotropic nonlocal self-focusing media", Opt. Lett. 30, 869 (2005).

[11] Desyatnikov A.S., Sagemerten N., Fischer R., Terhalle B., Träger D., Neshev D.N., Dreischuh A., Denz C., Krolikowski W., Kivshar Y.S., "Two-dimensional self-trapped nonlinear photonic lattices", Opt. Express 14 2851 (2006).

[12] Rosberg C.R., Neshev D.N., Sukhorukov A.A., Krolikowski W., Kivshar Y.S., "Observation of nonlinear self-trapping in triangular photonic lattices", Opt. Lett. 32, 397 (2007).

[13] Rosberg C.R., Garanovich I.L., Sukhorukov A.A., Neshev D.N., Krolikowski W., Kivshar Y.S., "Demonstration of all-optical beam steering in modulated photonic lattices", Opt. Lett. 31, 1498 (2006).

[14] Suntsov S., Makris K.G., Christodoulides D.N., Stegemann G.I., Hache, A., Morandotti R., Yang H., Salamo G., Sorel M., "Observation of discrete surface solitons", Phys. Rev. Lett. 96, 063901 (2006).

[15] Smirnov E., Rüter C. E., Kip D., Shandarova K., Shandarov V., "Light propagation in double periodic nonlinear photonic lattices in lithium niobate", Appl. Phys. B 88, 359 (2007).

[16] Desyatnikov A.S., Kivshar Y.S., Torner L., "Optical vortices and vortex solitons", Prog. Optics 47, 291-391 (2005).

[17] Louis P.J.Y., Ostrovskaya E.A., Kivshar Y.S., "Dispersion control for matter waves and gap solitons in optical superlattices", Phys. Rev. A 71, 02361 (2005).

[18] Rose P., Richter T., Terhalle B., Imbrock J., Kaiser F., Denz C., "Discrete and dipole-mode gap solitons in higher-order nonlinear photonic lattices", Appl. Phys. B 89, 521 (2007).

[19] Terhalle B., Desyatnikov A.S., Bersch C., Träger D., Tang L., Imbrock J., Kivshar Y.S., Denz C., "Anisotropic photonic lattices and discrete solitons in photorefractive media", Appl. Phys. B 86, 399 (2007).

[20] Krolikowski W., Ostrovskaya E.A., Weilnau C., Geisser M., McCarthy G., Kivshar Y.S., Denz C., Luther-Davies B., "Observation of Dipole-Mode Vector Solitons", Phys. Rev. Lett. 85, 1424 (2000).

[21] Rakuljic G.A., Leyva V., Yariv A., "Optical data storage by using orthogonal wavelength-multiplexed volume holograms", Opt. Lett. 17, 1471 (1992).

[22] Mok F. H., "Angle-multiplexed storage of 5000 holograms in lithium niobate", Opt. Lett. 18, 915 (1993).

[23] Denz C., Pauliat G., Roosen G., Tschudi T., "Volume hologram multiplexing using a deterministic phase encoding method", Opt. Commun. 85, 171 (1991).

[24] Taketomi Y., Ford J. E., Sasaki H., Ma J., Fainman Y., Lee S.H., "Incremental recording for photorefractive hologram multiplexing", Opt. Lett. 16, 1774 (1991).

[25] Bartal G., Cohen O., Buljan H., Fleischer J.W., Manela O., Segev M., "Brillouin zone spectroscopy of nonlinear photonic lattices", Phys. Rev. Lett. 94, 163902 (2005).

[26] Terhalle B., Träger D., Tang L., Imbrock J., Denz C., "Structure analysis of two-dimensional nonlinear self-trapped photonic lattices in anisotropic photorefractive media", Phys. Rev. E 74, 057601 (2006).

[27] Neshev D.N., Alexander T.J., Ostrovskaya E.A., Kivshar Y.S., Martin H., Makasyuk I., Chen Z., "Observation of Discrete Vortex Solitons in Optically Induced Photonic Lattices", Phys. Rev. Lett. 92, 123903 (2004).
[28] Fleischer J.W., Bartal G., Cohen O., Manela O., Segev M., Hudock J., Christodoulides D.N., "Observation of Vortex-Ring "Discrete" Solitons in 2D Photonic Lattices", Phys. Rev. Lett. 92, 123904 (2004).
[29] Tung S., Schweikhard V., Cornell E.A., "Observation of Vortex Pinning in Bose-Einstein Condensates", Phys. Rev. Lett. 97, 240402 (2006).
[30] Schweikhard V., Tung S., Cornell E.A., "Vortex Proliferation in the Berezinskii-Kosterlitz-Thouless Regime on a Two-Dimensional Lattice of Bose-Einstein Condensates", Phys. Rev. Lett. 99, 030401 (2007).
[31] Kevrekidis P.G., Malomed B.A., and Gaididei Y.B., "Solitons in triangular and honeycomb dynamical lattices with the cubic nonlinearity", Phys. Rev. E 66, 016609 (2002).
[32] Yang J., Musslimani Z.H., "Fundamental and vortex solitons in a two-dimensional optical lattice", Opt. Lett. 28, 2094 (2003).
[33] Baizakov B.B., Malomed B.A., Salerno M., "Multidimensional solitons in periodic potentials", Europhys. Lett. 63, 642 (2003).
[34] Yang J., "Stability of vortex solitons in a photorefractive optical lattice", New J. Phys. 6, 47 (2004).
[35] Bartal G., Manela O., Cohen O, Fleischer J.W., Segev M., "Observation of Second-Band Vortex Solitons in 2D Photonic Lattices", Phys. Rev. Lett. 95, 053904 (2005).
[36] Terhalle B., Richter T., Law K.J., Göries D., Rose P., Alexander T.J., Kevrekidis P.G., Desyatnikov A.S., Krolikowski W., Kaiser F., Denz C., Kivshar Y.S., "Observation of double-charge discrete vortex solitons in hexagonal photonic lattices", accepted for publication in Phys. Rev. A 2009.
[37] Alexander T.J., Desyatnikov A.S., Kivshar Y.S., "Multivortex solitons in triangular photonic lattices", Opt. Lett. 32, 1293 (2007).
[38] Alexander T.J., Sukhorukov A.A., Kivshar Y.S., "Asymmetric Vortex Solitons in Nonlinear Periodic Lattices", Phys. Rev. Lett. 93, 063901 (2004).
[39] Law K.J.H., Kevrekidis P. G., Alexander T.J., Krolikowski W., Kivshar Y.S., "Stable higher-charge discrete vortices in hexagonal optical lattices", Phys. Rev. A 79, 025801 (2009).
[40] Kartashov Y.V., Ferrando A., Egorov A.A., Torner L., "Soliton Topology versus Discrete Symmetry in Optical Lattices", Phys. Rev. Lett. 95, 123902 (2005).
[41] Cai L.Z., Yang X.L., Wang Y.R., "All fourteen Bravais lattices can be formed by interference of four noncoplanar beams", Opt. Lett. 27, 900-902 (2002).
[42] Dwivedi A., Xavier J., Joseph J., Singh K., "Formation of all fourteen Bravais lattices of three dimensional photonic crystal structures by a dual beam multiple-exposure holographic technique", Appl. Opt. 47, 1973-1980 (2008).